Please cite this article as: Singewald, K. *et al.* (2021). Copper Based Site-directed Spin Labeling of Proteins for Use in Pulsed and Continuous Wave EPR Spectroscopy. *Bio-protocol* 11(24): e4258. DOI: 10.21769/BioProtoc.4258.

bio-protocol www.bio-protocol.org/e4258 Bio-protocol 11(24): e4258. DOI:10.21769/BioProtoc.4258

Copper Based Site-directed Spin Labeling of Proteins for Use in Pulsed and Continuous Wave EPR Spectroscopy

Kevin Singewald, James A. Wilkinson, and Sunil Saxena*

Department of Chemistry, University of Pittsburgh, Pittsburgh, USA

*For correspondence: sksaxena@pitt.edu

[Abstract] Site-directed spin labeling in conjunction with electron paramagnetic resonance (EPR) is an attractive approach to measure residue specific dynamics and point-to-point distance distributions in a biomolecule. Here, we focus on the labeling of proteins with a Cu(II)-nitrilotriacetic acid (NTA) complex, by exploiting two strategically placed histidine residues (called the dHis motif). This labeling strategy has emerged as a means to overcome key limitations of many spin labels. Through utilizing the dHis motif, Cu(II)NTA rigidly binds to a protein without depending on cysteine residues. This protocol outlines three major points: the synthesis of the Cu(II)NTA complex; the measurement of continuous wave and pulsed EPR spectra, to verify a successful synthesis, as well as successful protein labeling; and utilizing Cu(II)NTA labeled proteins, to measure distance constraints and backbone dynamics. In doing so, EPR measurements are less influenced by sidechain motion, which influences the breadth of the measured distance distributions between two spins, as well as the measured residue-specific dynamics. More broadly, such EPR-based distance measurements provide unique structural constraints for integrative structural biophysics and complement traditional biophysical techniques, such as NMR, cryo-EM, FRET, and crystallography.

Graphic abstract:

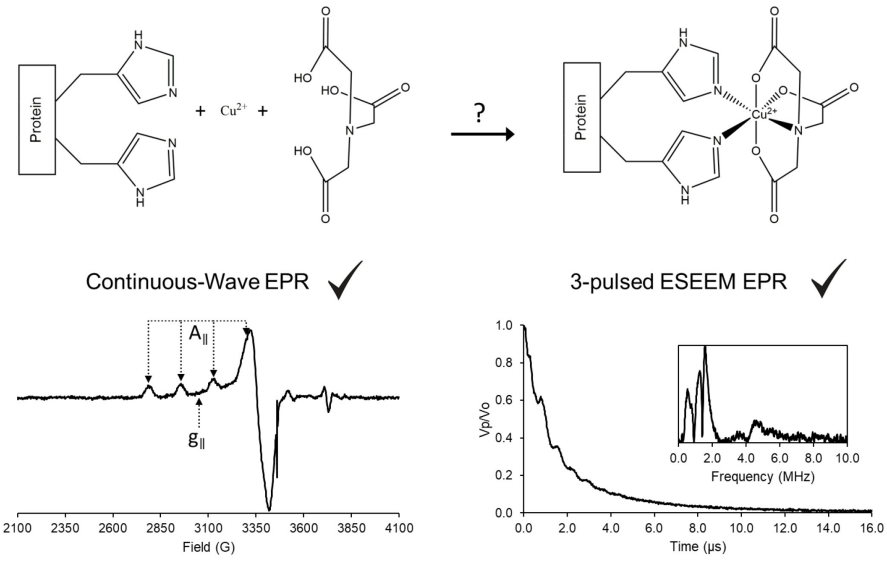

Monitoring the success of Cu(II)NTA labeling.

Please cite this article as: Singewald, K. *et al.* (2021). Copper Based Site-directed Spin Labeling of Proteins for Use in Pulsed and Continuous Wave EPR Spectroscopy. *Bio-protocol* 11(24): e4258. DOI: 10.21769/BioProtoc.4258.

Bio-protocol 11(24): e4258.
DOI:10.21769/BioProtoc.4258

Keywords: Spin Labeling, Copper, ESR, EPR, Continuous Wave, ESEEM, Dynamics

[Background] Electron paramagnetic resonance (EPR) holds a unique position in structural biology as it focuses on residue-specific information, rather than the global structure that other techniques strive for. The first focus of EPR employs pulsed strategies to provide nanometer-scale distance measurements between two or more spin labels. While multiple pulsed techniques exist, the most common method, which is double electron-electron resonance (DEER), works by flipping the spin of one electron spin and measuring its influence on another nearby spin (Pannier *et al.*, 2000). This information can be used incisively to measure induced conformational changes, locate binding sites, and establish quaternary structure, as well as the relative positioning of two biomolecules (Park *et al.*, 2006; Gaffney *et al.*, 2012; Jeschke, 2012). The other application of EPR in structural biology focuses on the relationship of protein function to site-specific dynamics. The EPR lineshape is sensitive to the tumbling rate of the paramagnetic species. Therefore, this lineshape provides information on residue specific motional rates (Hubbell *et al.*, 1998).

In order to use EPR, spin labeling is a key component as most biomolecules are diamagnetic, *i.e.*, EPR inactive (Todd *et al.*, 1989). In fact, spin labeling enables selective measurements with minimal to no background interference. Most spin labels utilize cysteine residues as attachment points to the protein (Klug *et al.*, 2021). However, labeling a specific cysteine may require other native cysteines to be mutated out, which can be problematic in many cases (Poole, 2015; Qiu *et al.*, 2015). Additionally, the intrinsic flexibility of most spin labels can influence the measured distance distribution between two spins, as well as the measured side-chain dynamics (Klose *et al.*, 2012). On the other hand, site-directed Cu(II) labeling to the double histidine motif (dHis) overcomes these limitations. This labeling is reliant on Cu(II) binding to two strategically placed histidine residues of a protein: i and i+2 for β-sheets, and for α-helices i and i+4. Furthermore, the use of the Cu(II)NTA complex enhances the selectively to the dHis motif, while minimizing native or non-specific Cu(II) binding (Ghosh *et al.*, 2018). The bi-pedal attachment of Cu(II)NTA to two His residues leads to distance distributions that can be up to 5-times narrower than traditional nitroxide labels (Cunningham *et al.*, 2015). Correspondingly, the dHis motif has been exploited to study subtle conformational changes that cannot be resolved with standard nitroxide radicals (Sameach *et al.*, 2019), locate native metal binding sites with fewer distance constraints (Gamble Jarvi *et al.*, 2019), and directly analyze backbone dynamics (Singewald *et al.*, 2020). On the other hand, this technique has not been thoroughly explored for buried regions in a protein or for membrane proteins. This protocol aims to outline Cu(II) labeling of proteins and how to monitor successful labeling.

Materials and Reagents

1. Mechanical micropipettes (Eppendorf, catalog number: 2231302001)
2. Matching pipette tips for the mechanical micropipettes (Fisher Scientific, catalog numbers: 02-707-507, 02-707-450, 02-717-133)

3. 1.5 ml Microcentrifuge tube (Eppendorf, catalog number: 022363204)
4. Conical tubes, 15 ml (Thermo Fisher Scientific, catalog number: 339650)
5. Quartz EPR tubes, 3 mm I.D. × 4 mm O.D. × 250 mm length (Sigma-Aldrich, catalog number: Z566535)
6. Quartz capillary tubes, 0.8 mm I.D. × 1 mm O.D. × 100 mm length (VitroCom, catalog number: CV8010-Q-100)
7. Capillary tube sealant (Fisher Scientific, catalog number: 02-678)
8. PTFE tape, medium density, 12.7 mm × 13.21 mm (Anti-Seize Technology, catalog number: 16035)
9. Dewar shielded vacuum flasks for freezing in liquid nitrogen, 350 ml (Pope Scientific, catalog number: 8600-0099)
10. Low form Dewar flask, 275 ml (Cole-Parmer, catalog number: EW-03771-21)
11. Metal wire, approximately 50 cm
12. Brass cylinder, 20 mm diameter × 30 mm length, with a blind hole on one end, 7 mm diameter × 25 mm length
13. Gas regulator (Uniweld, catalog number: RP3E)
14. Tygon E-3603 tubing, 5/16” I.D. × 7/16” O.D. (Cole-Parmer, catalog number: EW-07407-83)
15. Safety goggles (Fisher Scientific, catalog number: 12-888-305)
16. Cryogen protecting gloves (Grainger, catalog number: 2AEY6)
17. Deionized water (Fisher Scientific, catalog number: 21-520-113)
18. Copper sulfate pentahydrate (Spectrum Chemical, catalog number: C1431)
19. Hydrochloric acid, needed to prepare 1 M HCl solution for pH adjustment (Fisher Scientific, catalog number: 02003059)
20. Sodium hydroxide pellets, needed to prepare 1 M NaOH solution for pH adjustment (Fisher Scientific, catalog number: 56-753-0250GM)
21. Calibration solutions (pH = 4.00, 7.00, 10.00) (Fisher Scientific, catalog numbers: SB101-500, SB107-500, SB115-500)
22. pH electrode storage solution (Hanna Instruments, catalog number: HI70300)
23. pH electrode fill solution (Hanna Instruments, catalog number: HI7082)
24. pH electrode storage cap (Hanna Instruments, catalog number: HI740200)
25. Sodium chloride (Fisher Scientific, catalog number: BP3581)
26. MOPS (Fisher Scientific, catalog number: BP358)
27. Nitrilotriacetic acid disodium, NTA (Sigma-Aldrich, catalog number: N0128)
28. Glycerol (Sigma-Aldrich, catalog number: G7757)
29. Ficoll PM 70 (Fisher Scientific, catalog number: 45002020)
30. MAP-Pro Propylene/propane gas (Bernzomatic, catalog number: MG9)
31. Liquid nitrogen for CW-EPR and ESEEM experiments
32. Liquid helium for DEER/PELDOR experiments
33. Protein with one or more dHis mutations

34. 100 mM MOPS Buffer (see Recipes)

Note: Deuterated solvents may be used to increase the T_m relaxation time for experiments that require longer evolution times (Casto et al., 2021).

Equipment

1. Analytical balance (Denver Instruments, model: M-220D)
2. Vortex-Genie 2 (Scientific Industries, catalog number: SI-0236)
3. pH electrode (Hanna Instruments, catalog number: HI1332B)
4. pH meter, accumet AB150 (Fisher Scientific, catalog number: 13-636-AB150A)
5. Refrigerator 4°C
6. Freezer -20°C and -80°C
7. Spectrophotometer to determine protein concentration (Thermo Scientific, model: NanoDrop 2000)
8. Bruker ElexSys E680 CW/FT X-band spectrometer
9. Bruker ER4118-MD5 resonator
10. Bruker ER4122 SHQE-W1 high resolution resonator
11. Oxford ITC503 temperature controller
12. Oxford LLT 650 low loss transfer tube
13. Oxford CF935 dynamic continuous-flow cryostat

Software

1. MATLAB Version R2020b or later (The MathWorks Inc.) https://www.mathworks.com/
2. EasySpin toolbox for MATLAB, Version 5.2.30, available for free (Stoll and Schweiger, 2006) https://www.easyspin.org/
3. Bruker Xepr software provided with EPR spectrometer
4. NanoDrop 2000 program provided with spectrophotometer
5. A program to do NLSL.MOMD analysis, available for free (Budil *et al.*, 1996) https://www.acert.cornell.edu/index_files/acert_ftp_links.php
6. Xepr ESEEM program and example scripts for use in EasySpin and NLSL are available at https://github.com/SaxenaLab/Copper

Procedure

All solutions are made in deionized water unless otherwise stated. Any pH adjustments were done using 1 M HCl or 1 M NaOH solutions. Practically, we have found that a variety of buffers, such as phosphate, HEPES (4-(2-hydroxyethyl)-1-piperazineethanesulfonic acid), MOPS (3-(N-morpholino)propanesulfonic acid), and NEM (N-ethylmorpholine) buffers can be used. However, the use of Tris buffer degrades

Please cite this article as: Singewald, K. *et al.* (2021). Copper Based Site-directed Spin Labeling of Proteins for Use in Pulsed and Continuous Wave EPR Spectroscopy. *Bio-protocol* 11(24): e4258. DOI: 10.21769/BioProtoc.4258.

labeling. Of the buffers listed above, MOPS allowed for the highest Cu(II)NTA labeling efficiency (Gamble Jarvi *et al.*, 2020a). Therefore, all experiments described here were done in MOPS buffer. Nonetheless, the differences between most buffers are small, so another buffer may be used if it is imperative for the system. In addition, the protocol provides conditions for labeling at pH = 7.4, but the labeling is tolerant to pH between 6.4 and 8.4, and the presence of competing ions such as Zn(II)NTA (Wort *et al.*, 2021b). The step-by-step EPR spectrometer protocol is available elsewhere (Vicino *et al.*, 2021), as well as in the Bruker manual that comes with the EPR spectrometer. Therefore, we provide parameters and steps specific for Cu(II) in the following protocol. The EPR experiments discussed use relevant parameters for X-band frequencies (roughly 9.8 GHz). While each individual EPR experiment should be completed in one sitting, the CW-EPR, 3-pulsed ESEEM, and DEER do not have to be performed back-to-back.

A. Preparation of Cu(II)NTA
   1. Cu(II)NTA Synthesis
      a. Preparation of the stock solution of Cu(II)NTA complex is modified from previously published literature (Mehlenbacher *et al.*, 2015). This synthesis is not time sensitive and can be performed with breaks in between each step.
      b. Adjust the pH of approximately 5 ml deionized water (DI) water to 12.00 in a 15 ml conical tube. Prepare a 100 mM NTA stock solution by dissolving 23.49 mg of NTA per 1 ml of pH = 12.00 DI water (117.46 mg/5 ml). The NTA is acidic and alters the pH of the solution, so be sure to maintain a pH of 12 by adding NaOH to ensure the NTA dissolves.
      c. In a separate 15 ml conical tube, adjust the pH of 5 ml of DI water to 2.00. Dissolve $Cu(II)SO_4 \cdot 5H_2O$ in the pH = 2.00 DI water at a ratio of 4.99 mg per 1 ml of DI water (24.95 mg/5 ml). This is the 20 mM $Cu(II)SO_4$ stock solution.
      d. In a separate 15 ml conical tube, dilute a 1 ml aliquot of the 100 mM NTA stock to 5 ml (20 mM NTA) using the MOPS buffer (see Recipes). Slowly add in 5 ml of the 20 mM $Cu(II)SO_4$ stock solution. This makes the 10 mM Cu(II)NTA stock solution. The Cu(II)NTA solution is a deeper blue color than the $Cu(II)SO_4$, as seen in Figure 1A. **If the Cu(II)NTA solution has a blue precipitate in it**, then the synthesis was unsuccessful and more care should be taken with pH adjustments.
      e. Cu(II)NTA does not last forever. Either a new stock should be made every couple of months or aliquots should be frozen for long-term storage. Periodically check the CW-EPR spectrum for any observable changes, which might indicate that the Cu(II)NTA stock has degraded (see next section on CW-EPR setup). If any precipitate forms in the Cu(II)NTA solution, prepare or thaw a fresh batch and check the CW-EPR spectrum.
   2. CW-EPR of Cu(II)NTA Complex
      a. Sample Preparation
         i. In a 1.5 ml Eppendorf tube, prepare 100 µl of 200 µM Cu(II)NTA in MOPS buffer. Add 20 µl glycerol to serve as a cryoprotectant. Vortex the Eppendorf tube to mix the

Please cite this article as: Singewald, K. *et al.* (2021). Copper Based Site-directed Spin Labeling of Proteins for Use in Pulsed and Continuous Wave EPR Spectroscopy. *Bio-protocol* 11(24): e4258. DOI: 10.21769/BioProtoc.4258.

solution.

ii. In a separate Eppendorf tube, prepare 100 µl of 200 µM Cu(II)SO_4 in MOPS buffer. Add 20 µl glycerol and vortex.

iii. Pipette all 120 µl the Cu(II)NTA and Cu(II)SO_4 sample into separate quartz EPR tubes. Alternatively, the sample can be transferred to the EPR tube using a Hamilton syringe combined with PTFE tubing via a Luer lock attachment. Unlike with nitroxide radicals, the quartz background is easily distinguishable from the Cu(II) spectra. Furthermore, the use of quartz over borosilicate is due to quartz being less prone to shattering.

iv. **Carefully** shake the EPR tubes until the solutions are settled at the bottom.

v. Optional: Cover the open end of the EPR tube with a thin layer PTFE tape. This helps prevent ice build-up inside the EPR tube due to atmospheric water. This can also help prevent the sample from getting stuck in the resonator. Alternatively, the tube can be capped with a precision seal rubber septum.

vi. Pour enough liquid nitrogen into the 350 ml dewar to submerge the EPR sample solution. Freeze the EPR samples by placing them in liquid nitrogen. Note that using liquid nitrogen to freeze samples is slow and, therefore, faster procedures that reduce changes of protein conformation and/or dynamics are recommended for biomacromolecules (see Step B2e below). Despite adding glycerol as a cryoprotectant, **the EPR tube can shatter** when freezing, and therefore proper PPE (goggles and cryogen protecting gloves) is advised. The risk of tube shattering is decreased for samples with a higher percentage of cryoprotectant. Once the sample is frozen, it can be placed in a -80°C freezer for long term storage or run immediately.

b. CW-EPR

i. Cool the MD5 resonator down to 80 K using liquid nitrogen. Refer to the Bruker manual supplied with ElexSys E680 EPR spectrometer to tune and set up the CW-EPR experiment. Insert the Cu(II)SO_4 sample into the resonator and tune the spectrometer.

ii. After the EPR instrument is cooled to 80 K and tuned, set the parameters to:

1) Modulation frequency = 100 kHz
2) Modulation amplitude = 4 G
3) Modulation phase = determine in next step, start with 0
4) Harmonic = 1
5) Smooth points = 0
6) Receiver gain = 60 dB
7) Conversion time = 20.48 ms
8) Center field = 3100 G, note that different microwave frequencies might require a different center field to have adequate baseline around the spectrum
9) Sweep width = 2000 G
10) If possible, turn on quadrature detection

iii. First, determine the modulation phase. Run a quick CW-EPR experiment. If quadrature

Please cite this article as: Singewald, K. *et al.* (2021). Copper Based Site-directed Spin Labeling of Proteins for Use in Pulsed and Continuous Wave EPR Spectroscopy. *Bio-protocol* 11(24): e4258. DOI: 10.21769/BioProtoc.4258.

detection is on, phase the spectrum until the signal is real, *i.e.*, the signal in the imaginary is minimized (Processing → Transformations → Phase). Insert this phase into the modulation phase mentioned in Step A2b.ii.3). If quadrature detection is off, run the CW-EPR experiment at various phases, until the spectrum signal is minimized (this means everything is in the imaginary). Then, change the phase by 90° to have the signal be 100% real. If the signal is negative, then change the phase by another 180°.

iv. Once the spectrum is phased, signal average the CW-EPR experiment until an acceptable level of signal to noise. For reference, the data in Figure 1 was acquired for 60 scans or roughly 20 min.

v. Detune and remove the Cu(II)SO_4 sample, as outlined in the Bruker manual. Repeat Steps A2b.i-iv. for the Cu(II)NTA sample.

vi. Detune and remove the Cu(II)NTA sample. Repeat Steps A2b.i-iv with a blank sample. In this case, the blank contained 100 µl MOPS buffer and 20 µl glycerol. The noise level of the blank CW-EPR spectrum should be equivalent or less than the other spectra.

vii. Background subtract the two EPR spectra.

1) Set the Cu(II)SO_4 spectrum as the primary and the background as the secondary spectrum.
2) Align the background with similar features observed in the Cu(II) spectra. To align in XEPR, go to Processing → Transformations → Left/Right Shift. This is necessary, since subtle differences in frequency can cause the spectra to shift relative to one another. Figure 1C shows the aligned background signal.
3) Change the intensity of the background such that the intensity of background peaks matches those observed in the Cu(II)SO_4 spectra. Go to Processing → Algebra → Constant Operation.
4) Subtract the background signal from the Cu(II)SO_4. Go to Processing → Algebra → Primary - Secondary.
5) On the left of the XEPR window, go to Baseline Correction → Polynomial → Define Region. Highlight the baseline on the left and right of the Cu(II)SO_4 signal. Choose the smallest order polynomial that gives a good fit to the background and click Subtract Line. Figure 1D contains the background and baseline subtracted CW-EPR Cu(II) spectra.
6) If using quadrature detection, extract the real component Processing → Complex → Real Part. This is the CW-EPR spectrum that will be used for all analysis.
7) Repeat Steps 1)-6) with the Cu(II)NTA sample.
8) The two spectra should look different from each other. If the Cu(II)NTA looks similar to the Cu(II)SO_4 after background subtraction, then the Cu(II)NTA synthesis was incomplete and needs to be redone.

viii. See section A of Data analysis to simulate the CW-EPR spectra.

Please cite this article as: Singewald, K. *et al.* (2021). Copper Based Site-directed Spin Labeling of Proteins for Use in Pulsed and Continuous Wave EPR Spectroscopy. *Bio-protocol* 11(24): e4258. DOI: 10.21769/BioProtoc.4258.

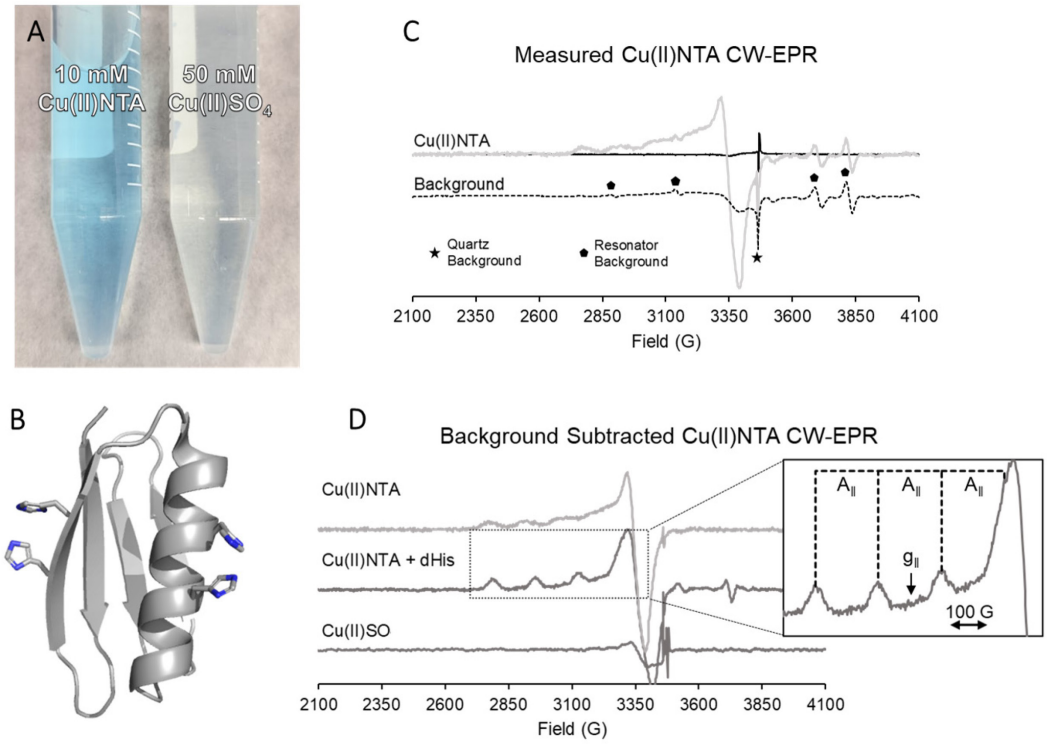

Figure 1. Preliminary Cu(II)NTA observations.

A. 10 mM Cu(II)NTA compared to 50 mM $Cu(II)SO_4$. Despite being a lower concentration, Cu(II)NTA has a deeper blue color than $Cu(II)SO_4$. This is an easy and crude way to confirm that the complexation has worked. B. Example positioning of the dHis motif is shown for an α-helical site (residues i and i+4) and a β-sheet site (residues i and i+2). The protein GB1 (pdb: 2QMT) was used for all sample data involving Cu(II)NTA labeled dHis. C. The raw CW-EPR spectra of Cu(II)NTA before any background subtraction is at the top (gray) with the blank sample CW-EPR below (black dashed). The black solid line overlayed with the Cu(II)NTA spectrum is the minimized imaginary component. Resonator signals are marked with pentagons and the quartz EPR tube signal is marked with a star. Note that, when annealed properly, higher purity quartz will have a less intense signal. The background spectra was shifted so these features are aligned. The Cu(II)NTA spectrum ranges from roughly 2,700 to 3,500 G. This is broader than a nitroxide spectra, therefore it is important to have a longer baseline on either side of the Cu(II) signal for adequate background subtraction. D. The background subtracted CW-EPR spectra for Cu(II)NTA ± dHis and $Cu(II)SO_4$ are shown. Note that the background subtraction is rarely perfect, due to subtle differences in the q-factor, experimental frequencies, and the fact that each sample uses a different quartz tube. However, the background subtraction should be as optimal as possible to avoid difficulties during analysis. The inset on the right points out two important features of any Cu(II) CW-EPR spectrum, $g_{||}$ (inversely proportional to the magnetic field) and the $A_{||}$ splitting (in Gauss).

B. Protein Labeling and Sample Preparation

1. Generate a mutant protein with one or two dHis mutations. To design a mutant protein, the secondary structure of the protein must be known. For α-helical sites, histidine mutations must be positioned on amino acid residues i and i+4. For β-sheet sites, histidine mutations are positioned on residues i and i+2 (Figure 1B). If the goal is to do dynamics measurements, then have one dHis mutation on the protein. For distance measurements between two sites, two dHis mutations are necessary, unless the protein forms an oligomer. Refer to previous work regarding expression and purification of proteins (Gräslund *et al.*, 2008).
2. Protein labeling
   a. In a 1.5 ml Eppendorf tube, prepare a 100 µl sample containing 200 µM Cu(II)NTA and 200 µM dHis (for example, 100 µM monomer with two dHis sties) in MOPS buffer. To determine protein concentration, a simple way to estimate the molar absorptivity can be found online (https://web.expasy.org/protparam/). Since the labeling reaction is exothermic (Wort *et al.*, 2019), it is important to incubate at 4°C for about 30 min. The labeling time may be influenced by the labeling site and can be accurately determined by UV-Vis spectroscopy (Gamble Jarvi *et al.*, 2020a).
   b. Add 20 µl glycerol and vortex. The glycerol prevents crystallization during freezing. In addition to preventing the EPR tube from shattering, glycerol allows the sample to freeze in a glass-like state which allows for longer T_m relaxation times (Casto *et al.*, 2021).
   c. Use a micropipette or Hamilton syringe with PTFE tubing to transfer the 120 µl protein sample into separate EPR tubes. **Carefully** shake the EPR tubes until the solution is settled at the bottom.
   d. Optional: Cover the open end of the EPR tube with PTFE tape or a precision seal rubber septum.
   e. Freeze the sample in precooled propylene + propane (MAP-Pro), see Figure 2 for freezing setup. This freezes the sample faster than submerging in liquid nitrogen for two reasons. Firstly, liquid nitrogen will always be at its boiling temperature. As such, anything warmer when submerged in liquid nitrogen will cause the nitrogen to boil. This creates a gas shield that provides poor thermal contact with the sample, known as the Leidenfrost effect (Walker, 2010). Because MAP-Pro is cooled below its boiling point, it will not boil when a warm sample is submerged in it. Furthermore, MAP-Pro has a similar heat capacity to liquid nitrogen. Alternatively, the sample can be cooled in liquid nitrogen, but this is a slower process and can allow the protein to adopt its most stable conformation, rather than all conformations at physiological temperatures (Georgieva *et al.*, 2012). Faster freezing methods, such as submerging in liquified ethane (Russo *et al.*, 2016), or rapid freeze-quench (Hett *et al.*, 2021), also eliminate this concern.

Please cite this article as: Singewald, K. *et al.* (2021). Copper Based Site-directed Spin Labeling of Proteins for Use in Pulsed and Continuous Wave EPR Spectroscopy. *Bio-protocol* 11(24): e4258. DOI: 10.21769/BioProtoc.4258.

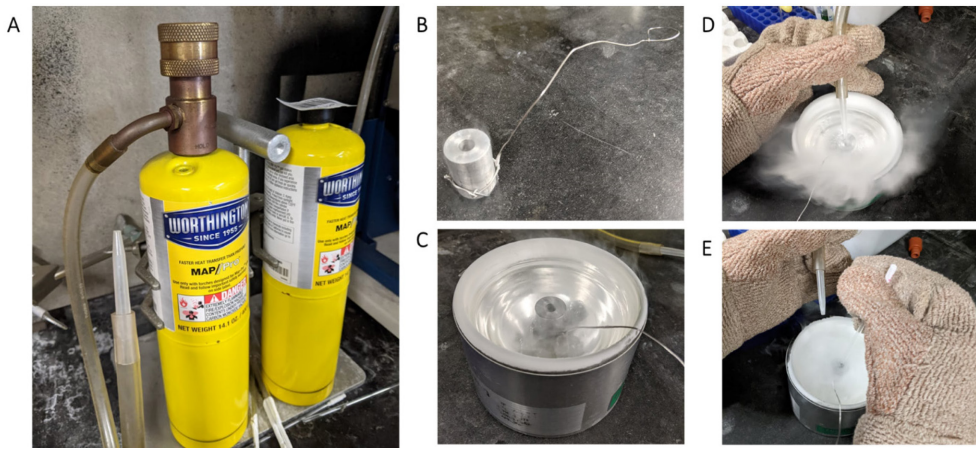

Figure 2. The EPR tube sample freezing setup.

See Video 1 for more information on the freezing protocol. A. MAP-Pro gas cylinder with RP3E gas regulator. Attached is the 5/16” I.D. tubing with a pipette tip inserted. B. Metal cylinder with blind hole used to freeze the sample. A metal wire is wound around the metal cylinder and used as a handle to safely move the cold metal. C. The metal cylinder is pre-cooled in liquid nitrogen. Wait for the nitrogen to stop rapid boiling before introducing MAP-Pro. Be sure that any liquid nitrogen on the inside of the metal cylinder is emptied as well. D. Open the MAP-Pro gas canister until gas is coming out. Be mindful of the gas flow rate: too slow of a flow rate will cause too much time to pass before enough MAP-Pro is liquified, and result in the MAP-Pro freezing in the metal cylinder; too fast of a flow rate will cause a large excess of gas to be pumped into the atmosphere; a good flow rate will cause a cloud to barely obstruct the view of the hole in the metal cylinder, as seen in the Figure above. Insert the MAP-Pro gas into the hole and blow or wave away the cloud to see the cylinder. Once the cylinder is filled with liquid, around **30 s at most**, insert the EPR sample for about one second. Remove the frozen EPR sample and place into a separate dewar filled with liquid nitrogen.

Video 1. Flash freezing the EPR sample.

Please cite this article as: Singewald, K. *et al.* (2021). Copper Based Site-directed Spin Labeling of Proteins for Use in Pulsed and Continuous Wave EPR Spectroscopy. *Bio-protocol* 11(24): e4258. DOI: 10.21769/BioProtoc.4258.

C. EPR Experiments on Cu(II)NTA labeled protein

1. Obtaining Anisotropic CW-EPR Spectrum
   a. Follow the protocol from Step A2b.
   b. Expected g_{II} and A_{II} values for Cu(II)NTA bound to dHis in MOPS are outlined in section A of Data analysis. Note that these values can change when Cu(II)NTA is in different buffers (Gamble Jarvi *et al.*, 2020a). Go to section A of Data analysis to simulate the CW-EPR spectrum. Obtain the labeling efficiency by simulating the CW-EPR spectrum with free and bound Cu(II)NTA. The labeling efficiency can be calculated from the simulated spectrum using the following equation:

$$\left(\frac{weight_{bound}}{weight_{bound} + weight_{free}}\right) \times 100\%$$

   Alternatively, the labeling efficiency can be calculated from the DEER modulation depth (Lawless *et al.*, 2017; Gamble Jarvi *et al.*, 2020b). Labeling efficiency can also be obtained from K_D curves obtained from UV-Vis (Gamble Jarvi *et al.*, 2020a) and RIDME pulsed EPR experiments (Wort *et al.*, 2021a).
2. Pulsed EPR preliminary experiments
   a. Cool the MD5 resonator down to 80 K with liquid nitrogen.
   b. Refer to the Bruker manual on pulsed experiment setup. Additionally, a useful protocol including preliminary pulsed experiments outlined in more detail was previously published (Vicino *et al.*, 2021). Run a field-swept spectrum with the center field and sweep width equal 3,100 G and 2,000 G (Figure 3A).
   c. Run a nutation experiment at the field of maximum intensity, to determine the optimal pulse lengths for future experiments (Figure 3B). Xepr can only do even length pulses, so change the attenuation until the π/2 pulse length is even.
   d. Run an echo decay experiment, also known as a 2-pulsed ESEEM experiment (Figure 3C). If ESEEM modulations do not dominate the signal, then fit the time domain signal to a stretched exponential decay to obtain the T_m relaxation time.
      In the PulseSPEL window, load the inversion recovery experiment (InvRec_ESE.exp) in the following folder:
      xeprFiles/PulseSPEL/shared/Standard/Spel2009/Relaxation
   e. Use the following parameters for the inversion recovery experiment (units are in ns unless otherwise stated): n = 1, d30 = 2000, d1 = 200, d2 = 1000, SRT = 1500 us, h = 10, p0 = π/2 pulse length determined in Step C2c, p1 = π pulse length determined in Step C2c, p2 = π pulse length, d0 and pg determination are outlined by Vicino *et al.* (2021).
      After the inversion recovery is finished, calculate T_1 following the information in Figure 3D. The shot rep time (SRT) used in all other 80 K pulsed experiments is equal to 5 × T_1.

Please cite this article as: Singewald, K. *et al.* (2021). Copper Based Site-directed Spin Labeling of Proteins for Use in Pulsed and Continuous Wave EPR Spectroscopy. *Bio-protocol* 11(24): e4258. DOI: 10.21769/BioProtoc.4258.

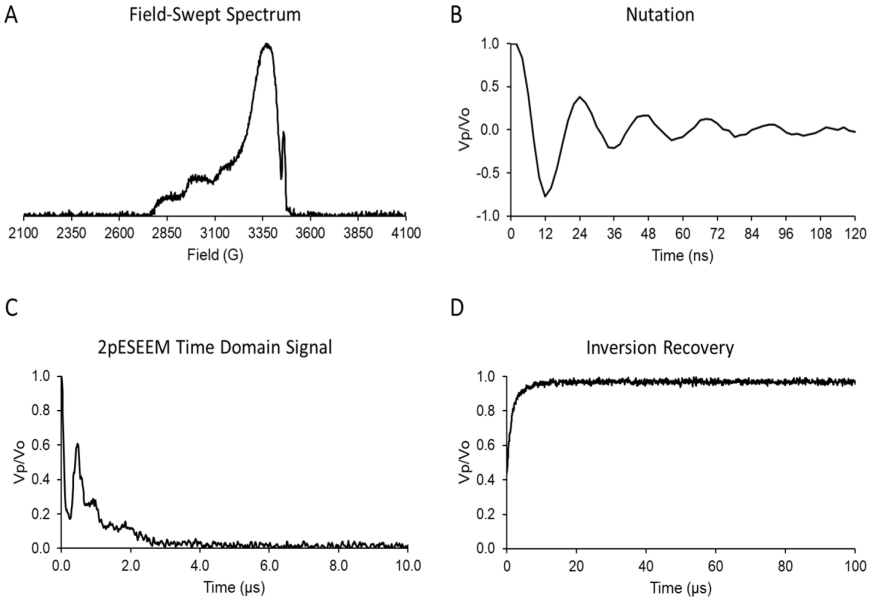

Figure 3. Pulsed EPR data necessary for all other pulsed techniques.

A. The echo detected field-swept spectra of Cu(II)NTA bound to dHis. Experiments are performed at the maximum intensity of approximately 3,350 G. B. Nutation experiment to determine the optimal pulse lengths for efficient spin inversion. The first of the minima is the π-pulse length, in this case 12 ns. The π/2 pulse length is therefore 6 ns. C. The echo decay (2pESEEM) time domain signal is shown. This experiment is useful to determine the maximum dipolar evolution time allowed in DEER experiments due to T_m, the phase memory relaxation time. Make note of when the echo decay is at a baseline, as this represents the time limit of the DEER pulse sequence. For this sample, the baseline is around 3 µs. Therefore, pulse sequences longer than 3 µs are unlikely to produce an adequate echo in DEER. Unlike with nitroxide radicals, nitrogen ESEEM often dominates the echo decay, so fitting with a stretched exponential decay to determine T_m can be difficult. If T_m is desired, one way to overcome this issue is to use softer pulses to weaken the ESEEM modulations. D. The inversion recovery sequence for Cu(II)NTA at 80 K is shown. This experiment is important to measure the necessary SRT used in future experiments. The SRT applies a delay between every measured data point to ensure spin relax back to equilibrium. An SRT equal to 5 times the longitudinal relaxation time (T_1) allows for 99% of the spin magnetization to recover between each experiment. T_1 can be determined by fitting the inversion recovery to the following equation: $Intensity = A(1 - 2e^{(\tau/T_1)^\gamma})$. A is the amplitude, γ is a stretch parameter between 0 and 1, and τ is the pulse separation (the x-axis variable in the time domain signal). Vary A, T_1, and γ until the fit is optimal. **The EPR instrument has a minimum SRT**, so if the measured SRT is too short, lengthen the SRT until the error message disappears. The above data was acquired with an SRT = 400 µs.

3. Three Pulsed Electron Spin Echo Envelop Modulation (3pESEEM)
   a. Download the ESEEM program and parameters file from GitHub (see Software).
   b. In the acquisition tab of the parameters window, check “Run from PulseSPEL” and open the PulseSPEL window.
   c. Click “Load Var. Def.” and load the variable definitions file “ESEEMvar.def” downloaded in Step C3a. Click “Compile” in the PulseSPEL window. Then click “Load Program” and load the 3pESEEM.exp file. Click “Compile” again.
   d. In the Parameters window, set both the experiment and phase cycling to “3pESEEM setup”. Enter in the following parameters into the PulseSPEL variable textbox (units default to ns unless otherwise stated).
      i. d0 = 0
      ii. pg = 0
      iii. d1 ≈ 148, depending on the magnetic field. This value is important in running experiments at the hydrogen blind spot. To calculate the optimal d1, download the excel document located on GitHub. Note that pulses are nonideal, in other words, have a nonzero duration and therefore a finite frequency bandwidth. As such, it may be necessary to try a few values around the calculated d1 to optimize the hydrogen ESEEM suppression.
      iv. d2 = 288
      v. dx = 0, dy = 0
      vi. d30 = 16
      vii. p1 is the π pulse length determined in Step C2c.
      viii. p0 is half of p1. Both of these numbers need to be even.
      ix. SRT is determined in Step C2e. Be sure to add “us” after the number since the units are not in ns (for example: 500 us).
      x. n = 1
      xi. a = 1024
      xii. h = 100
   e. In the PulseSPEL window, click Validate. If no errors appear, then run the setup experiment. Errors usually appear if the experiment was not switched to PulseSPEL mode (Step C3b) or if the program detects parameters which are illogical. Be sure that everything is input correctly. Another possible error can occur if the pulse sequence exceeds the memory of the spectrometer. This can be solved by lowering the step size, d30, or decreasing the number of points at the top of the script.
   f. Check the phase of the 3pESEEM echo. If the echo is not phased, change the signal phase in the FT Bridge window under the Receiver Unit tab. Continue to change the phase and rerun the setup until everything is real and positive. Find the start of the echo (d0) and the width of the echo (pg). Set these values in the PulseSPEL variable textbox.

Please cite this article as: Singewald, K. *et al.* (2021). Copper Based Site-directed Spin Labeling of Proteins for Use in Pulsed and Continuous Wave EPR Spectroscopy. *Bio-protocol* 11(24): e4258. DOI: 10.21769/BioProtoc.4258.

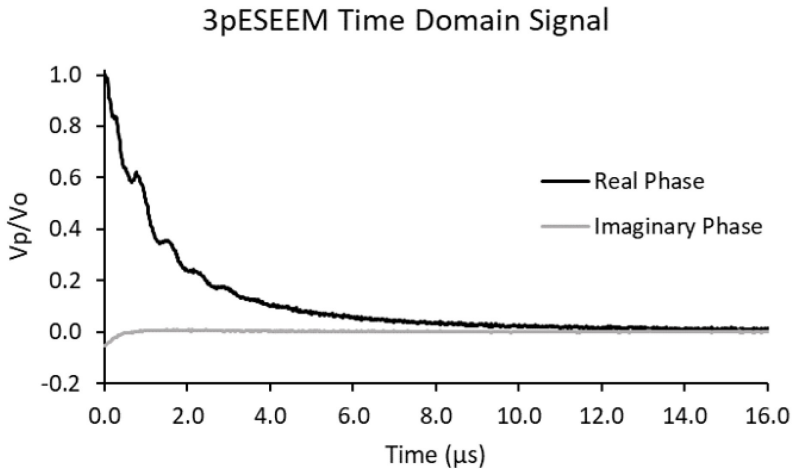

Figure 4. The real and imaginary phase for the 3pESEEM time domain signal. The real component (black) is what should be used in all future experiments. The imaginary component (gray) should be phased such that no modulations are present.

g. Change the experiment and phase cycling to "3pESEEM". Click validate in the PulseSPEL window. If no errors appear, then set the number of scans (n) to an arbitrarily large value (for example n = 10000) and run the 3pESEEM experiment. If an error appears, go back and be sure that all parameters are entered in correctly. The 3pESEEM experiment takes roughly 12 h to acquire adequate signal to noise at 80 K, but might be shorter or longer depending on labeling efficiency, the total number of Cu(II) atoms, and the pulse length. Alternatively, the 3pESEEM can be obtained at 18 K, usually in under 1 h.

h. Once the 3pESEEM is ready to be stopped, set n to be 1 higher than the current number of scans. This allows the current scan to finish without interruption. Phase the time domain signal such that all the modulations are in the real phase. Sometimes, the phasing is not perfect and signal remains in the imaginary component (Figure 4). If this is the case, then the Fourier transform will show an intense peak at zero frequency. To prevent this, go to Processing → Complex → Real part.

i. See section B under Data analysis for more information on 3pESEEM.

4. Double Electron-Electron Resonance (DEER)/Pulsed Electron Double Resonance (PELDOR)

   a. The DEER setup and analysis was previously outlined (Vicino *et al.*, 2021). This protocol will only discuss differences in setup from the work described on nitroxide radicals. For proteins that are unstable at higher concentrations, distance measurements from relaxation-induced dipolar modulation enhancement (RIDME) can be obtained at sub-micromolar concentrations (Ackermann *et al.*, 2021).

   b. Cool the MD5 resonator down to 18 K with liquid helium.

   c. Insert the EPR sample into the MD5 resonator and tune following the Bruker manual.

   d. Follow Steps C2b-e at 18 K before setting up the DEER experiment.

Please cite this article as: Singewald, K. *et al.* (2021). Copper Based Site-directed Spin Labeling of Proteins for Use in Pulsed and Continuous Wave EPR Spectroscopy. *Bio-protocol* 11(24): e4258. DOI: 10.21769/BioProtoc.4258.

e. Set the center field to the maximum intensity observed in the field-swept spectrum, roughly 3,350 G.
f. Run nutation experiments at two frequencies that are 150 MHz apart. The lower frequency will be the pump frequency (ν_B) and the higher frequency is the observer frequency (ν_A). These pulses should be as short as possible, to maximize the excitation bandwidth of the pulse.
g. Rerun the field-swept spectrum at ν_B. Set the center field to the maximum intensity. Then change the frequency to ν_A.
h. Continue to follow the protocol by Vicino *et al*. (2021) to run the DEER experiment. When setting up the DEER, be sure to account for the maximum allowed dipolar evolution time determined from the echo decay experiment (Step C2d).

5. Room Temperature Dynamics Measurements
   a. Prepare 25 µl of 300 µM Cu(II)NTA and 900 µM protein in MOPS. Underloading the protein with Cu(II)NTA ensures that the resulting CW-EPR spectra has a negligible component of free Cu(II)NTA. For smaller proteins (<50 kDa), the sample can contain 25% w/v Ficoll in order to slow down global tumbling and minimize its influence on the CW-EPR lineshape (López *et al.*, 2009).
   b. Draw up the solution into the quartz capillary tube via capillary action and seal the same end with capillary tube sealant. Insert the capillary into the 250 mm length quartz tube and insert this into the SHQE high resolution resonator.
   c. Setup and tune the spectrometer following the Bruker manual.
   d. Set the CW-EPR parameters to:
      i. Modulation frequency = 100 kHz
      ii. Modulation amplitude = 6 G
      iii. Modulation phase = determine in next step, start with 0
      iv. Harmonic = 1
      v. Smooth points = 0
      vi. Receiver gain = 60 dB
      vii. Conversion time = 20.48 ms
      viii. Center field = 3200 G, note that different microwave frequencies might require a different center field to have adequate baseline around the spectrum
      ix. Sweep width = 1600 G
      x. If possible, turn on quadrature detection
   e. Similar to Step A2b.iii, determine the modulation phase. If the signal is too weak to quickly find the modulation phase, then run the experiment at phase = 0 and phase afterwards.
   f. Run the CW-EPR experiment until adequate signal to noise ratio, roughly 12 h.
   g. Repeat Steps C5a-C5f with MOPS buffer to obtain a background spectrum.
   h. Follow Steps A2b.vii to background subtract the CW-EPR spectrum. Repeat these steps with free Cu(II)NTA or Cu(II)NTA + wild type protein to confirm that acquired spectrum

Please cite this article as: Singewald, K. *et al.* (2021). Copper Based Site-directed Spin Labeling of Proteins for Use in Pulsed and Continuous Wave EPR Spectroscopy. *Bio-protocol* 11(24): e4258. DOI: 10.21769/BioProtoc.4258.

contains dHis-bound Cu(II)NTA.

i. See section C of Data analysis to simulate the room temperature CW-EPR spectra.

Data analysis

A. Analysis of 80 K CW-EPR spectra

1. Crudely calculate the g_{II} and A_{II} for the Cu(II)NTA spectrum. The expected values for g_{II} and A_{II} are outlined in Figure 5. These values can differ when the Cu(II)NTA complex is in different buffer solutions.

$$g \approx \frac{Microwave\ Frequency\ (MHz)}{1.4 \times Magnetic\ field\ (G)}$$

A_{II} can be measured from the peak splitting outlined in Figure 1.

2. Use the EasySpin toolbox in MATLAB (Stoll and Schweiger, 2006) to simulate the Cu(II)NTA and dHis bound Cu(II)NTA spectra. Scripts to simulate Cu(II) CW-EPR spectra that can be used in EasySpin are available on GitHub (see Software section). The EasySpin script identifies all parameters and necessary information, so minimal MATLAB knowledge is required. Fit the spectra with the manual fitting code before the automatic fitting, to ensure that the automatic fitting code does not get stuck in a local minimum and generate a poor fit. The two Cu(II) spectra should be fit with different parameters. If the dHis bound Cu(II)NTA requires additional components, try simulating with parameters obtained from free Cu(II)NTA to check if complexation was complete. Similarly, it is possible to fit the $Cu(II)SO_4$ CW-EPR spectrum to compare to Cu(II)NTA to see if complexation was complete.

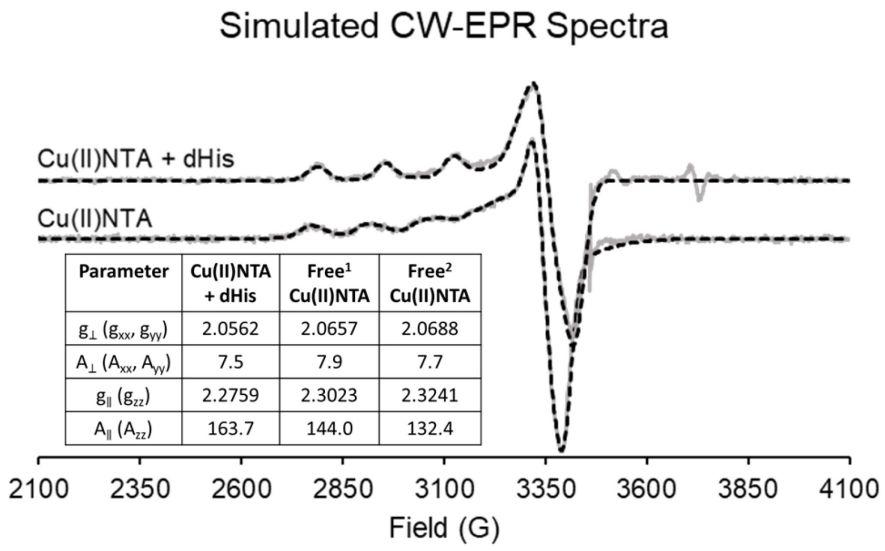

Parameter	Cu(II)NTA + dHis	Free[1] Cu(II)NTA	Free[2] Cu(II)NTA
$g_{\perp}$ (g_{xx}, g_{yy})	2.0562	2.0657	2.0688
$A_{\perp}$ (A_{xx}, A_{yy})	7.5	7.9	7.7
$g_{\parallel}$ (g_{zz})	2.2759	2.3023	2.3241
$A_{\parallel}$ (A_{zz})	163.7	144.0	132.4

Figure 5. EasySpin simulated CW-EPR spectra.

The CW-EPR spectra for Cu(II)NTA with dHis (top) and without dHis (bottom) are shown. These

Please cite this article as: Singewald, K. *et al.* (2021). Copper Based Site-directed Spin Labeling of Proteins for Use in Pulsed and Continuous Wave EPR Spectroscopy. *Bio-protocol* 11(24): e4258. DOI: 10.21769/BioProtoc.4258.

were obtained first by doing a manual simulation to position the peaks, and then allowing the automatic fitting script to finish the fit. The free Cu(II)NTA required two components to obtain an adequate fit, likely due to multiple coordination geometries of NTA to the Cu(II) atom (Gamble Jarvi *et al.*, 2020a). The table shows relevant parameters used to fit the data. Hyperfine values $A_{\perp}$ and A_{II} are in Gauss. Be aware that $A_{\perp}$ is too small to observe for these samples and therefore $A_{\perp}$ is often ambiguous from line broadening parameters.

B. 3pESEEM

1. Fit the 3pESEEM time domain signal to either a stretched exponential decay or biexponential decay, whichever gives a better fit. Subtract out the exponential decay as shown in Figure 6A.
2. Go to Processing → Transformations → FFT and click Transform. Then go to Processing → Complex → Absolute to obtain the 3pESEEM spectrum. If the Fourier transform has an intense signal at 0 frequency, then the background subtraction needs to be redone. Try to use different exponential fits, or utilize a region qualifier to only fit the featureless tail of the 3pESEEM time domain signal.
3. Cu(II) bound to dHis has a unique 3pESEEM spectrum compared to other coordination sites (Figure 6B). The nuclear quadrupole interaction (NQI) occurs at frequencies of 0.5, 1.0, and 1.5 MHz (Shin and Saxena, 2011). The double quantum (DQ) frequency is around 4-5 MHz. **Check for frequencies around 2.8 MHz, as this is indicative of backbone coordination**.

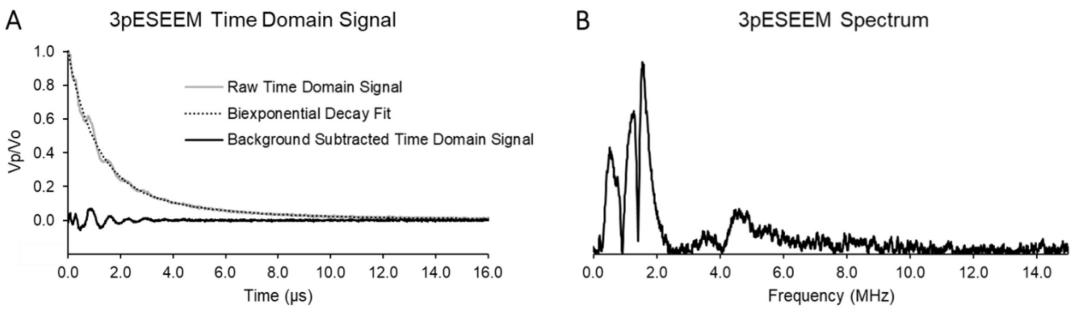

Figure 6. 3pESEEM analysis.

A. The 3pESEEM time domain for Cu(II)NTA coordinated to dHis is shown. The background (black dotted) of the 3pESEEM time domain signal (gray solid) was fit with a biexponential decay. The background subtracted time domain is shown in black. B. Fourier transform of the background subtracted time domain signal. This has peaks consistent with dHis coordination. Note that the three NQI peaks (~1 MHz) are not always as well resolved.

C. Room temperature CW-EPR spectra

1. For specifics on understanding simulations using Nonlinear-Least-Squares Levenberg-Marquardt analysis (NLSL) of macroscopically disordered membrane domains (MOMD), see previously published work (Budil *et al.*, 1996).

2. When simulating room temperature Cu(II) spectra, use the following parameters:
   a. Input parameters determined from the experiment and from the simulated anisotropic spectrum. This includes gxx, gyy, gzz, Axx, Ayy, Azz, and b0.
   b. Let in2 = 3
   c. Let betad = 90
   d. Let nort = 20
   e. Basis set parameters:
      lemx = 20
      lomx = 19
      kmx = 10
      mmx = 6
      ipnmx = 4
   f. Vary c20, gib0, and rbar.
   g. As starting values, let c20 = 1, gib0 = 40, and rbar = 8

Recipes

1. 100 mM MOPS Buffer
   45 ml deionized water
   1.05 g MOPS
   0.29 g NaCl
   Adjust pH to 7.4
   Dilute to 50 ml with deionized water

Acknowledgments

This research was funded by National Science Foundation (NSF BSF MCB-2006154). This protocol should be read in conjunction with our recent review (Gamble Jarvi *et al.*, 2021). This protocol builds off of previous research articles from the Saxena group on Cu(II) labeling (Ghosh *et al.*, 2018; Gamble Jarvi *et al.*, 2020a) and room temperature dynamics measurements (Singewald *et al.*, 2020).

Competing interests

The authors declare no competing interests nor conflicts of interest.

References

1. Ackermann, K., Wort, J. L. and Bode, B. E. (2021). Nanomolar Pulse Dipolar EPR Spectroscopy

in Proteins: Cu^{II}-Cu^{II} and Nitroxide-Nitroxide Cases. *J Phys Chem B* 125(20): 5358-5364.

2. Budil, D. E., Lee, S., Saxena, S. and Freed, J. H. (1996). Nonlinear-Least-Squares Analysis of Slow-Motion EPR Spectra in One and Two Dimensions Using a Modified Levenberg–Marquardt Algorithm. *J Magn Reson, Ser A* 120(2): 155-189.
3. Casto, J., Mandato, A. and Saxena, S. (2021). dHis-troying Barriers: Deuteration Provides a Pathway to Increase Sensitivity and Accessible Distances for Cu^{2+} Labels. *J Phys Chem Lett* 12(19): 4681-4685.
4. Cunningham, T. F., Putterman, M. R., Desai, A., Horne, W. S. and Saxena, S. (2015). The double-histidine Cu^{2+}-binding motif: a highly rigid, site-specific spin probe for electron spin resonance distance measurements. *Angew Chem Int Ed Engl* 54(21): 6330-6334.
5. Gaffney, B. J., Bradshaw, M. D., Frausto, S. D., Wu, F., Freed, J. H. and Borbat, P. (2012). Locating a lipid at the portal to the lipoxygenase active site. *Biophys J* 103(10): 2134-2144.
6. Gamble Jarvi, A., Bogetti, X., Singewald, K., Ghosh, S. and Saxena, S. (2021). Going the dHis-tance: Site-Directed Cu^{2+} Labeling of Proteins and Nucleic Acids. *Acc Chem Res* 54(6): 1481-1491.
7. Gamble Jarvi, A., Casto, J. and Saxena, S. (2020a). Buffer effects on site directed Cu^{2+}-labeling using the double histidine motif. *J Magn Reson* 320: 106848.
8. Gamble Jarvi, A., Cunningham, T. F. and Saxena, S. (2019). Efficient localization of a native metal ion within a protein by Cu^{2+}-based EPR distance measurements. *Phys Chem Chem Phys* 21(20): 10238-10243.
9. Gamble Jarvi, A., Sargun, A., Bogetti, X., Wang, J., Achim, C. and Saxena, S. (2020b). Development of Cu^{2+}-Based Distance Methods and Force Field Parameters for the Determination of PNA Conformations and Dynamics by EPR and MD Simulations. *J Phys Chem B* 124(35): 7544-7556.
10. Georgieva, E. R., Roy, A. S., Grigoryants, V. M., Borbat, P. P., Earle, K. A., Scholes, C. P. and Freed, J. H. (2012). Effect of freezing conditions on distances and their distributions derived from Double Electron Electron Resonance (DEER): a study of doubly-spin-labeled T4 lysozyme. *J Magn Reson* 216: 69-77.
11. Ghosh, S., Lawless, M. J., Rule, G. S. and Saxena, S. (2018). The Cu^{2+}-nitrilotriacetic acid complex improves loading of α-helical double histidine site for precise distance measurements by pulsed ESR. *J Magn Reson* 286: 163-171.
12. Gräslund, S., Nordlund, P., Weigelt, J., Hallberg, B. M., Bray, J., Gileadi, O., Knapp, S., Oppermann, U., Arrowsmith, C., Hui, R., Ming, J. *et al*. (2008). Protein production and purification. *Nat Methods* 5(2): 135-146.
13. Hett, T., Zbik, T., Mukherjee, S., Matsuoka, H., Bonigk, W., Klose, D., Rouillon, C., Brenner, N., Peuker, S., Klement, R., *et al*. (2021). Spatiotemporal Resolution of Conformational Changes in Biomolecules by Combining Pulsed Electron-Electron Double Resonance Spectroscopy with Microsecond Freeze-Hyperquenching. *J Am Chem Soc* 143(18): 6981-6989.
14. Hubbell, W. L., Gross, A., Langen, R. and Lietzow, M. A. (1998). Recent advances in site-

directed spin labeling of proteins. *Curr Opin Struct Biol* 8(5): 649-656.

15. Jeschke, G. (2012). DEER distance measurements on proteins. *Annu Rev Phys Chem* 63: 419-446.
16. Klose, D., Klare, J. P., Grohmann, D., Kay, C. W., Werner, F. and Steinhoff, H. J. (2012). Simulation vs. reality: a comparison of in silico distance predictions with DEER and FRET measurements. *PLoS One* 7(6): e39492.
17. Klug, C., Lerch, M. and Feix, J. (2021). Applications of Nitroxide Spin Labels to Structural Biology. In: *Nitroxides*. Ouari, O. and Gigmes, D. (Eds.). 392-419.
18. Lawless, M. J., Ghosh, S., Cunningham, T. F., Shimshi, A. and Saxena, S. (2017). On the use of the Cu^{2+}–iminodiacetic acid complex for double histidine based distance measurements by pulsed ESR. *Phy Chem Chem Phys* 19(31): 20959-20967.
19. López, C. J., Fleissner, M. R., Guo, Z., Kusnetzow, A. K. and Hubbell, W. L. (2009). Osmolyte perturbation reveals conformational equilibria in spin-labeled proteins. *Protein Sci* 18(8): 1637-1652.
20. Mehlenbacher, M. R., Bou-Abdallah, F., Liu, X. X. and Melman, A. (2015). Calorimetric studies of ternary complexes of Ni(II) and Cu(II) nitrilotriacetic acid and N-acetyloligohistidines. *Inorganica Chim Acta* 437: 152-158.
21. Pannier, M., Veit, S., Godt, A., Jeschke, G. and Spiess, H. W. (2000). Dead-time free measurement of dipole-dipole interactions between electron spins. *J Magn Reson* 142(2): 331-340.
22. Park, S. Y., Borbat, P. P., Gonzalez-Bonet, G., Bhatnagar, J., Pollard, A. M., Freed, J. H., Bilwes, A. M. and Crane, B. R. (2006). Reconstruction of the chemotaxis receptor-kinase assembly. *Nat Struct Mol Biol* 13(5): 400-407.
23. Poole, L. B. (2015). The basics of thiols and cysteines in redox biology and chemistry. *Free Radic Biol Med* 80: 148-157.
24. Qiu, H., Honey, D. M., Kingsbury, J. S., Park, A., Boudanova, E., Wei, R. R., Pan, C. Q. and Edmunds, T. (2015). Impact of cysteine variants on the structure, activity, and stability of recombinant human alpha-galactosidase A. *Protein Sci* 24(9): 1401-1411.
25. Russo, C. J., Scotcher, S. and Kyte, M. (2016). A precision cryostat design for manual and semi-automated cryo-plunge instruments. *Rev Sci Instrum* 87(11): 114302.
26. Sameach, H., Ghosh, S., Gevorkyan-Airapetov, L., Saxena, S. and Ruthstein, S. (2019). EPR Spectroscopy Detects Various Active State Conformations of the Transcriptional Regulator CueR. *Angew Chem Int Ed Engl* 58(10): 3053-3056.
27. Shin, B. K. and Saxena, S. (2011). Substantial contribution of the two imidazole rings of the His13-His14 dyad to Cu(II) binding in amyloid-β(1-16) at physiological pH and its significance. *J Phys Chem A* 115(34): 9590-9602.
28. Singewald, K., Bogetti, X., Sinha, K., Rule, G. S. and Saxena, S. (2020). Double Histidine Based EPR Measurements at Physiological Temperatures Permit Site-Specific Elucidation of Hidden Dynamics in Enzymes. *Angew Chem Int Ed Engl* 59(51): 23040-23044.

29. Stoll, S. and Schweiger, A. (2006). EasySpin, a comprehensive software package for spectral simulation and analysis in EPR. *J Magn Reson* 178(1): 42-55.
30. Todd, A. P., Cong, J., Levinthal, F., Levinthal, C. and Hubbell, W. L. (1989). Site-directed mutagenesis of colicin E1 provides specific attachment sites for spin labels whose spectra are sensitive to local conformation. *Proteins* 6(3): 294-305.
31. Vicino, M. F., Hett, T. and Schiemann, O. (2021). Spin Labeling of RNA Using “Click” Chemistry for Coarse-grained Structure Determination via Pulsed Electron-electron Double Resonance Spectroscopy. *Bio-protocol* 11(9): e4004.
32. Walker, J. (2010). Boiling and the Leidenfrost effect. *Fundamentals of physics*: E10-11.
33. Wort, J. L., Ackermann, K., Giannoulis, A., Stewart, A. J., Norman, D. G. and Bode, B. E. (2019). Sub-Micromolar Pulse Dipolar EPR Spectroscopy Reveals Increasing Cu^{II}-labelling of Double-Histidine Motifs with Lower Temperature. *Angew Chem Int Ed Engl* 58(34): 11681-11685.
34. Wort, J. L., Ackermann, K., Norman, D. G. and Bode, B. E. (2021a). A general model to optimise Cu^{II} labelling efficiency of double-histidine motifs for pulse dipolar EPR applications. *Phys Chem Chem Phys* 23(6): 3810-3819.
35. Wort, J. L., Arya, S., Ackermann, K., Stewart, A. J. and Bode, B. E. (2021b). Pulse Dipolar EPR Reveals Double-Histidine Motif Cu^{II}-NTA Spin-Labeling Robustness against Competitor Ions. *J Phys Chem Lett* 12(11): 2815-2819.

